

# An analysis of Finite-Volume Schemes: High-order Methods and Grid Reflections on Adaptive Grids

Christiane Jablonowski  
Paul Ullrich  
*University of Michigan*

IPAM Workshop II, April 16, 2010

# Outline

- High-order Finite Volume methods for atmospheric flows
  - Cubed sphere grid
  - Shallow Water (SW) equations in conservation form
  - MUSCL-type Finite Volume schemes
    - Sub-grid-scale reconstruction
    - Riemann solvers
    - Discretization of the source terms
    - Discretization of interior boundaries & panel edges
  - Results of shallow water test cases
- Towards variable-resolution meshes and AMR
- Wave reflection properties and grid staggerings (1D SW)
- Path forward: 3D AMR with Chombo, cyclone tests

# The Cubed Sphere Grid

- The cubed sphere grid is obtained by placing a cube inside the sphere and “inflating” it to occupy the total volume of the sphere.
- We use the gnomonic equiangular cubed-sphere grid (recall Peter’s talk).
- Pros:
  - Removes polar singularities
  - Grid faces are individually regular
- Cons
  - Some difficulty handling edges
  - Multiple coordinate systems



# Shallow Water Equations

- The shallow water equations can be obtained from the vertically integrated Euler equations with a free surface. They represent the flow of a single layer of fluid, with or without topography
- The orthonormal conservation form with source terms is:

$$\begin{aligned}\frac{\partial h}{\partial t} + \frac{\partial}{\partial x}(hu) + \frac{\partial}{\partial y}(hv) &= 0 \\ \frac{\partial(hu)}{\partial t} + \frac{\partial}{\partial x}\left(hu^2 + \frac{1}{2}Gh^2\right) + \frac{\partial}{\partial y}(huv) &= \Psi_{M,x} + \Psi_{C,x} + \Psi_{T,x} \\ \frac{\partial(hv)}{\partial t} + \frac{\partial}{\partial x}(huv) + \frac{\partial}{\partial y}\left(hv^2 + \frac{1}{2}Gh^2\right) &= \Psi_{M,y} + \Psi_{C,y} + \Psi_{T,y}\end{aligned}$$

G: gravity

h: height of free surface

u,v: zonal and meridional velocity

Metric

Topography

Coriolis

# Shallow Water Equations

- The more general, compact form of the conservation law is

$$\frac{\partial \vec{q}(\vec{x}, t)}{\partial t} + \frac{1}{\sqrt{g}} \frac{\partial}{\partial x^k} \vec{F}^k = \vec{\Psi}_M(\vec{q}, \vec{x}) + \vec{\Psi}_C(\vec{q}, \vec{x}) + \vec{\Psi}_T(\vec{q}, \vec{x})$$

$$\vec{q}(\vec{x}, t) = \begin{pmatrix} h \\ hu^1 \\ hu^2 \end{pmatrix} : \text{state vector with directional indices } 1, 2$$

$\vec{F}$  : flux vector

$\vec{\Psi}(\vec{q}, \vec{x})$  : source terms due to the metric, Coriolis force, topography

$\sqrt{g}$  : square root of metric determinant

$$\begin{pmatrix} \mathbf{u} \\ \mathbf{v} \end{pmatrix} = \mathbf{O} \begin{pmatrix} u^1 \\ u^2 \end{pmatrix} \text{ with orthonormalization matrix } \mathbf{O}$$

# Shallow Water Equations

- Idea behind the Finite Volume scheme: integrate the shallow water conservation laws over a given element  $Z$  with area  $|Z|$  and apply the Gauss' divergence theorem

$$\frac{\partial \bar{q}}{\partial t} + \frac{1}{|Z|} \oint_{\partial Z} \vec{F}^k dl = \bar{\Psi}_M + \bar{\Psi}_C + \bar{\Psi}_T$$

with volume - average :  $\bar{\Phi} = \frac{1}{|Z|} \int_Z \Phi dV$

$dl$  is a line segment along the boundary  $\partial Z$

# Why Finite Volumes?

- Finite volume methods have several advantages over finite difference and spectral methods:
  - They can be used to **conserve invariant quantities**, such as mass, energy, potential vorticity or potential enstrophy.
  - Finite volume methods do not suffer from “spectral ringing” and generally only realize “physically attainable” states (no spurious increases in entropy).
  - Finite volume methods can be easily made to satisfy **monotonicity** and **positivity** constraints (i.e. to avoid negative tracer densities).

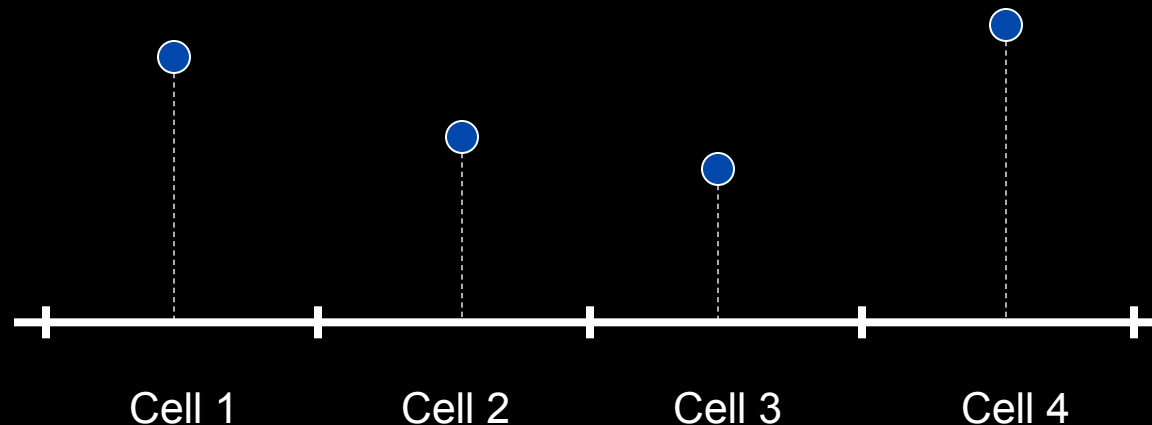
# Finite Volume Formulation

- A Monotone Upstream-centered Scheme for Conservation Laws (MUSCL)-type finite volume scheme on the cubed-sphere consists of three parts:
  - 1 A sub-grid-scale reconstruction (can be made monotonic)
  - 2 A Riemann solver
  - 3 A discretization of the source terms

# Finite Volume Formulation

1

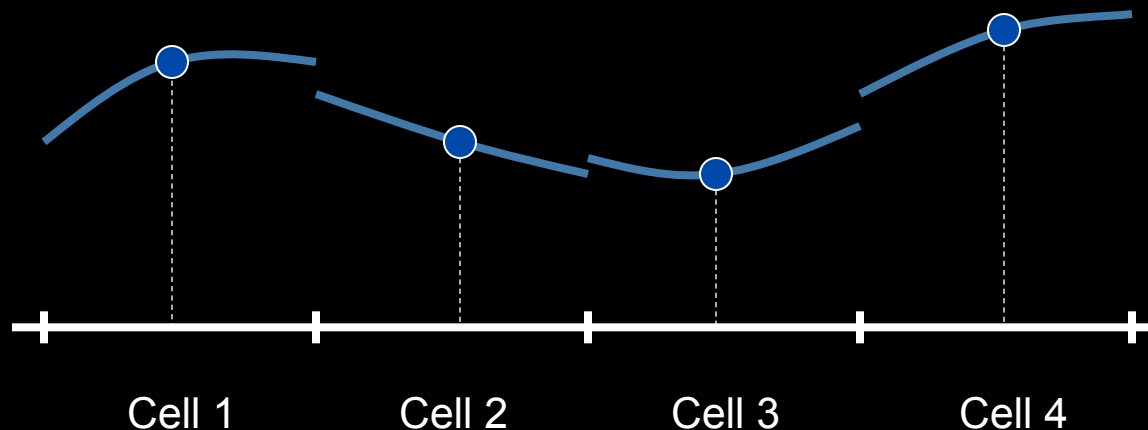
The finite volume formulation relies on only the cell-averaged values within each element in order to obtain a description of the sub-grid-scale behavior (recall Alistair's talk).



# Sub-Grid Scale Reconstruction

1

We make use of polynomial reconstructions (third and fourth-order) within each element in order to represent the mass and momentum on the sub-grid scale (recall Alistair's talk).



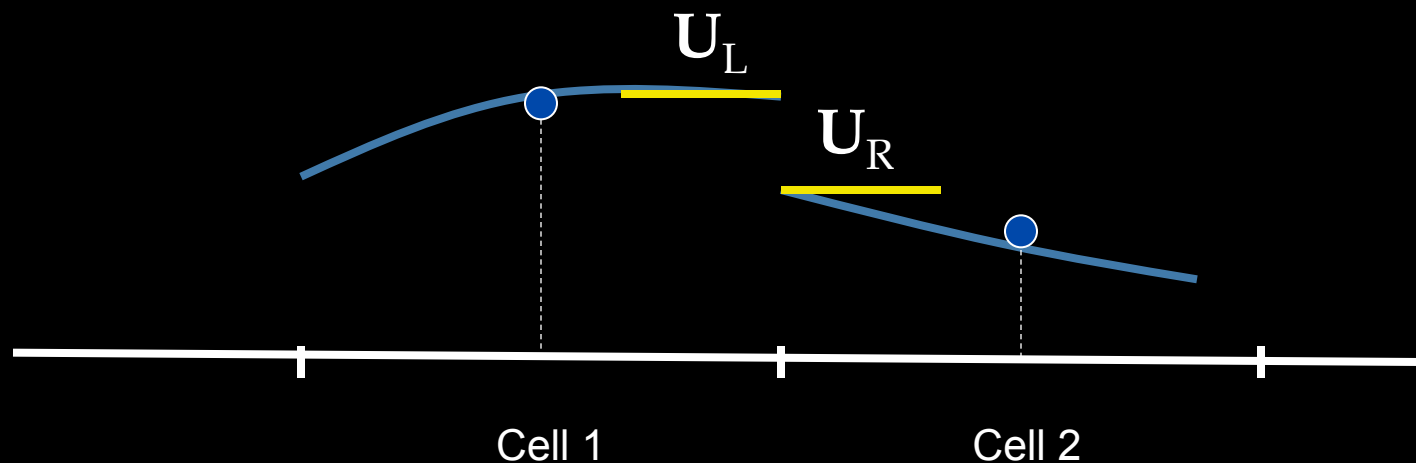
Examples are: Piecewise Parabolic Method (PPM) to achieve 3<sup>rd</sup> order (FV3)  
Piecewise Cubic Method (PCM) to achieve 4<sup>th</sup> order (FV4)

# The Riemann Solver

2

Since the reconstruction is inherently discontinuous at cell interfaces, we must solve a Riemann problem to obtain the flux of all conserved variables (recall Vincent's talk).

$$\mathbf{U}(x, t = 0) = \begin{cases} \mathbf{U}_L & \text{if } x < 0 \\ \mathbf{U}_R & \text{if } x > 0 \end{cases}$$



# The Riemann Solver

## 2

Solving the Riemann problem exactly is generally computationally expensive, and so we must make use of approximate Riemann solvers.

The **Rusanov Riemann solution (also called Lax-Friedrichs flux)** is simplest and least computationally intensive, but most diffusive. Local propagation speed: maximum eigenvalue of the flux Jacobian matrix.

The **Roe Riemann solver** (Roe, 1981) breaks up the flux into a set of waves and determines the relative strength and speed of each wave. This method is popular for aerospace problems (shocks), but is still diffusive for low Mach number flows.

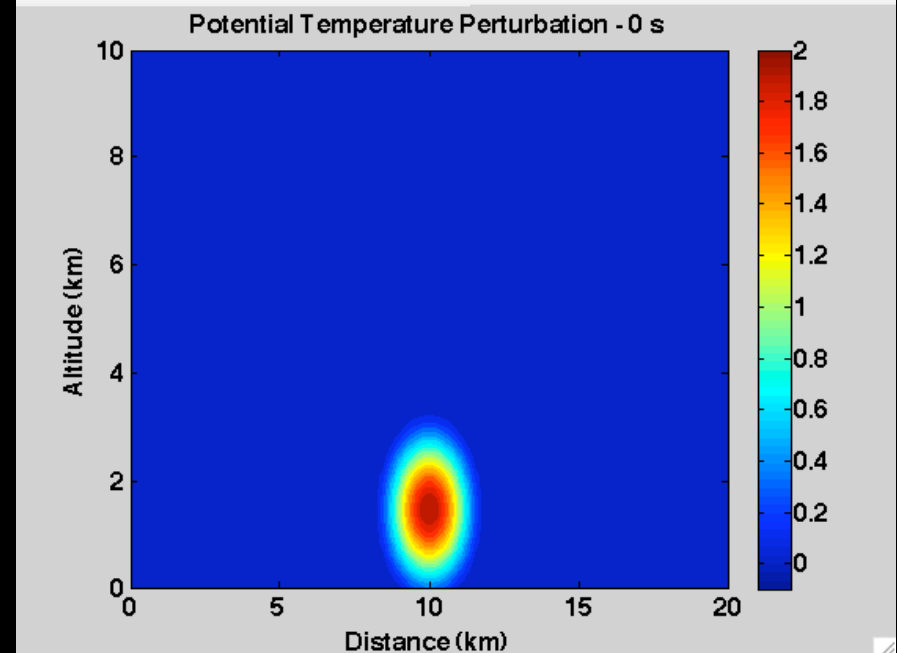
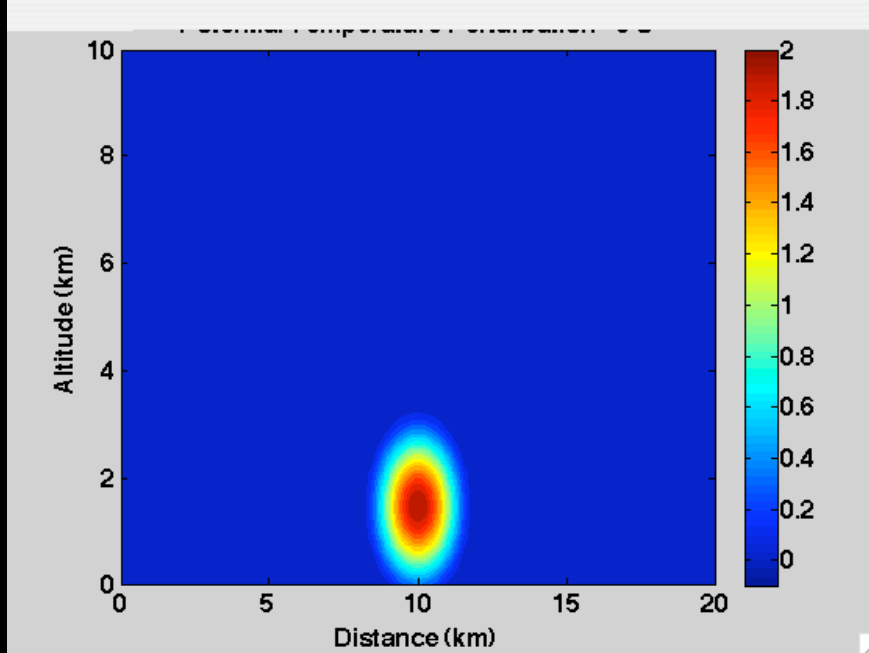
A variant of the 'Advection Upstream Splitting Method' called **AUSM<sup>+</sup>-up Riemann solver** (Liou, JCP 2006) is the most computationally intensive, but provides very accurate results for low-speed flows. Splits the advective component of the flux from the pressure component.

# The Riemann Solver

2

FV schemes with 3<sup>rd</sup> or 4<sup>th</sup> order accuracy are sensitive to the diffusive properties of the approximate Riemann solver. Higher-order DG schemes with 8<sup>th</sup> or 16<sup>th</sup> order accuracy are insensitive to their diffusive properties (Frank's experience).

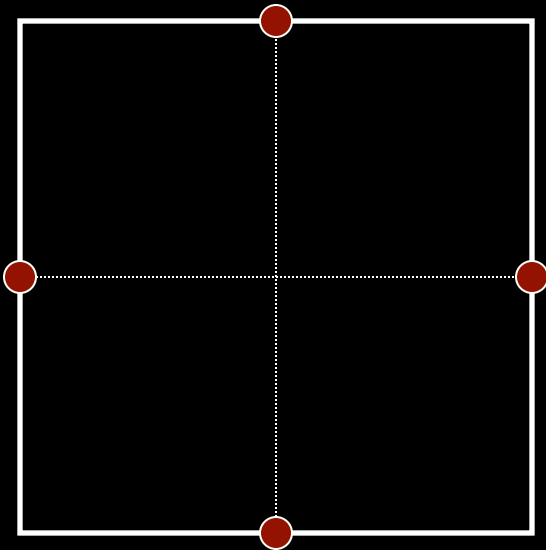
Warm bubble: Potential temperature perturbation in 4<sup>th</sup>-order FV  
Rusanov AUSM<sup>+</sup>-up



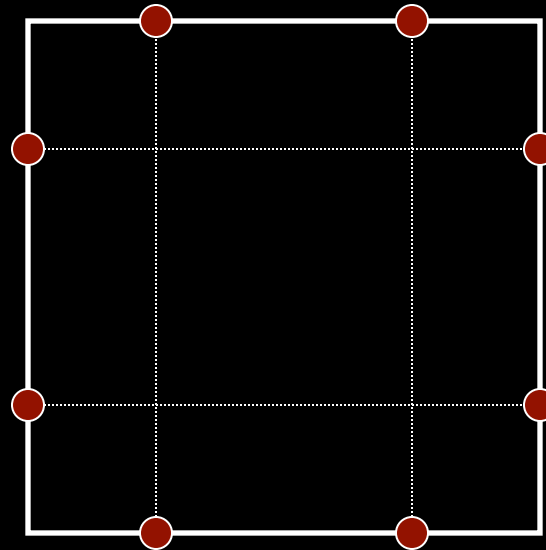
# The Riemann Solver

2

In 2D we must guarantee that the line integral for the flux is calculated with adequate precision. Since Gaussian quadrature guarantees the highest order accuracy with the fewest evaluations, we will use it to compute the flux along each edge.



One Gaussian quadrature point per edge is required for 2nd order accuracy.

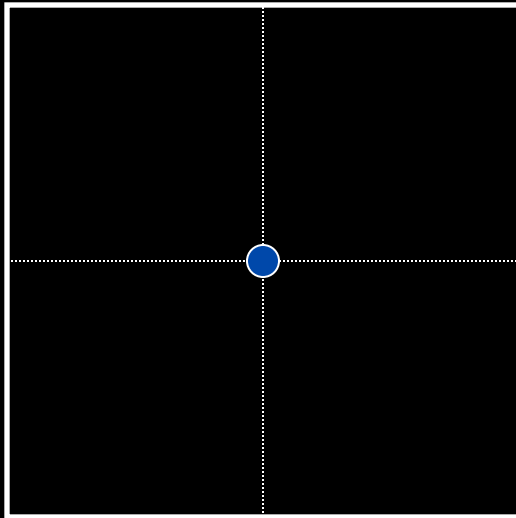


Two Gaussian quadrature points per edge are required for 4th order accuracy.

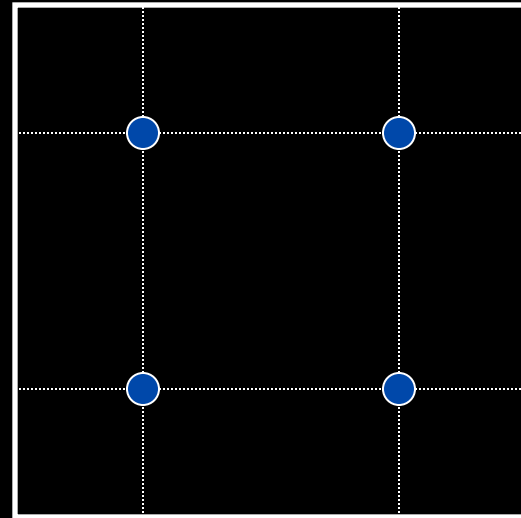
# Source Terms

3

Source terms are similarly easily discretized using Gaussian quadrature on the interior of each element to ensure high-order accuracy.



One Gaussian quadrature point is required to guarantee 2nd order accuracy.

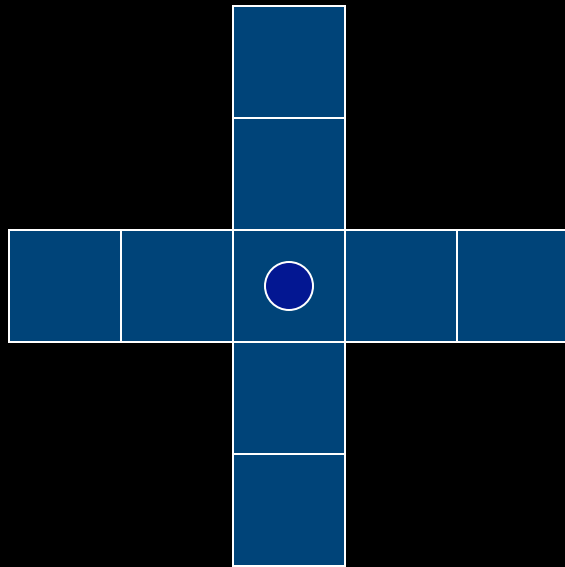


Four Gaussian quadrature points are required to guarantee 4th order accuracy.

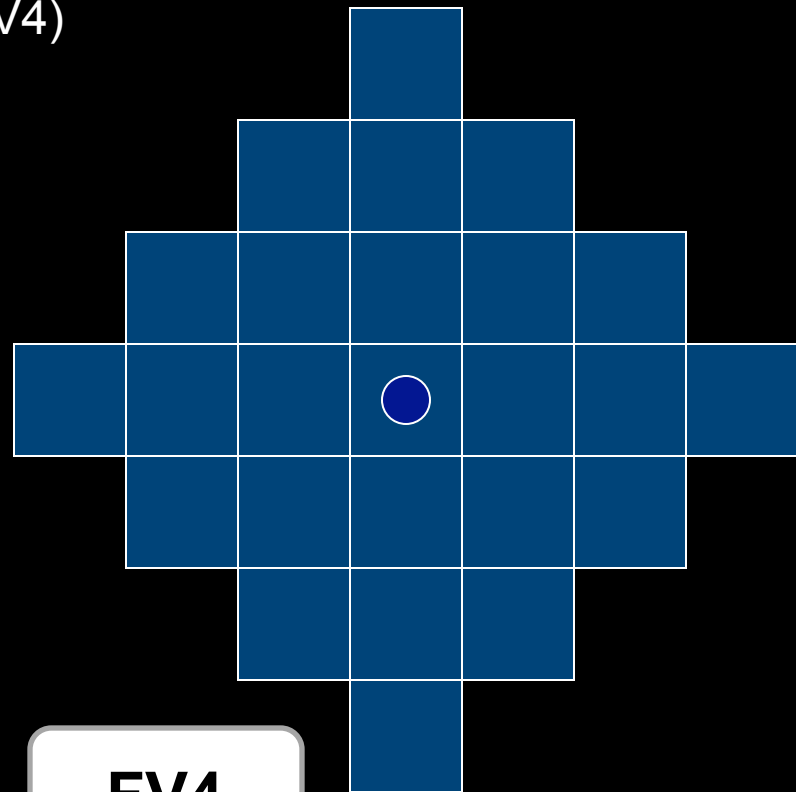
# Schemes

We test two schemes under this model:

- A piecewise-parabolic method (FV3) with dimension-split stencil
- A piecewise-cubic method (FV4)



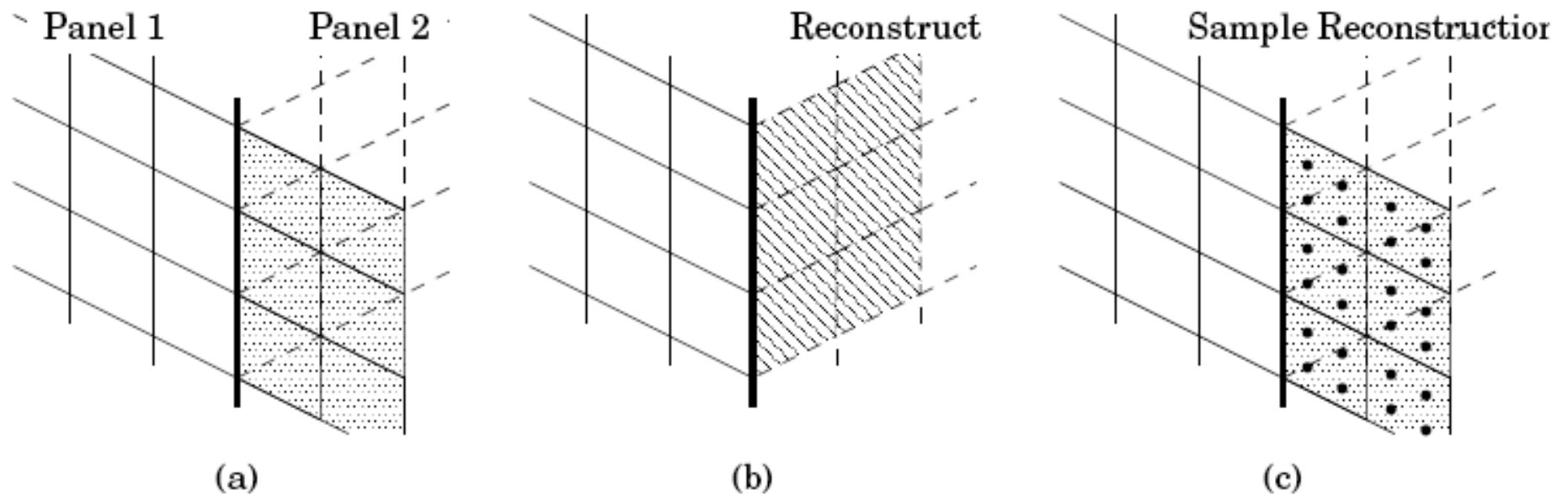
**FV3**



**FV4**

# Boundary Treatment

- At cubed-sphere panel edges ghost cells need to be filled.
- This is done via one-sided PPM-type reconstructions on the source grid (panel 2) that are sampled at 4 Gauss points on the destination grid (panel 1).

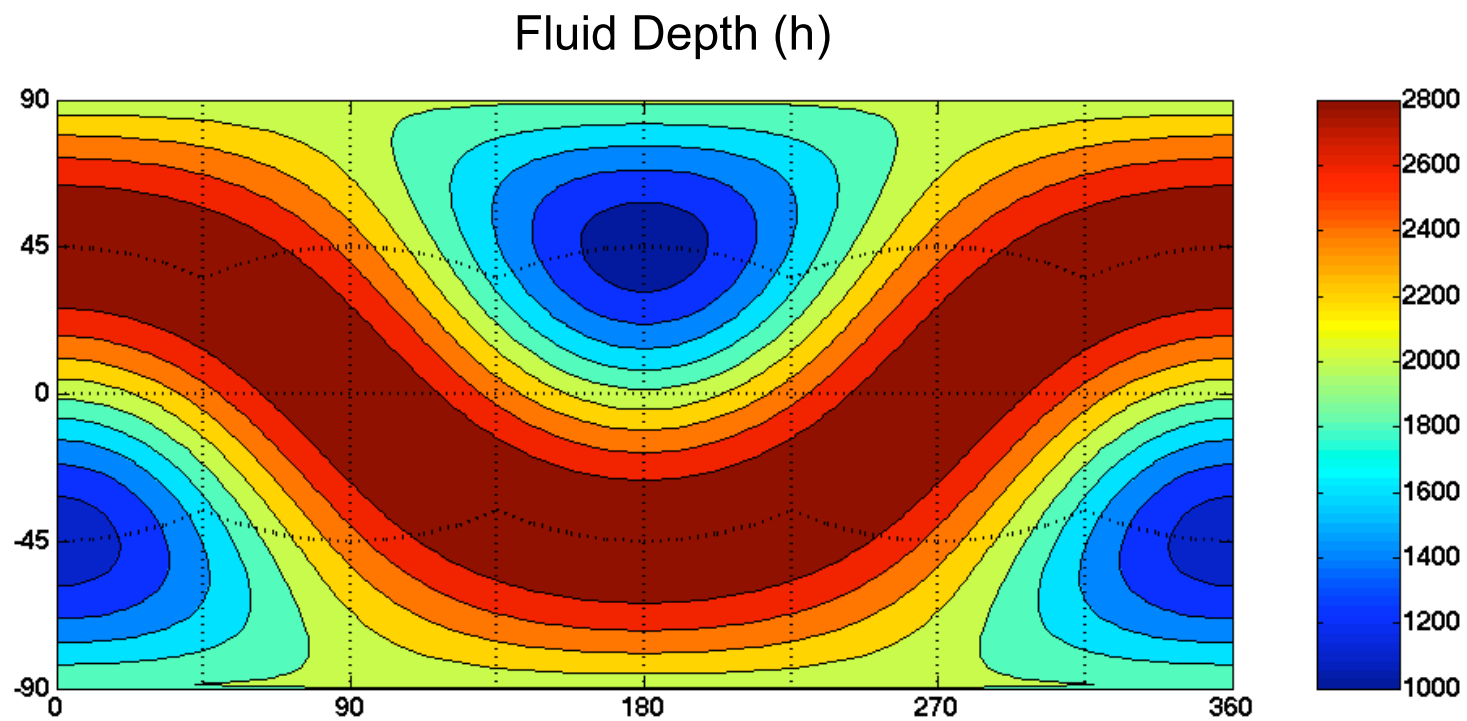


# Other Design Choices

- Unstaggered A-grid
- 3<sup>rd</sup> and 4<sup>th</sup>-order Runge-Kutta time stepping method paired with FV3 and FV4, allows CFL > 1
- No limiters, under- and overshoots are possible (limiters will be necessary for tracer advection)
- We mainly show experiments at the resolutions:
  - 40x40x6 ( $\approx 2.25^\circ$  deg or 250 km)
  - 80x80x6 ( $\approx 1.1^\circ$  deg or 125 km)
  - 120x120x6 ( $0.75^\circ$  deg or 83 km)
- All details in Ullrich, Jablonowski, van Leer, JCP, revised (4/15/2010)

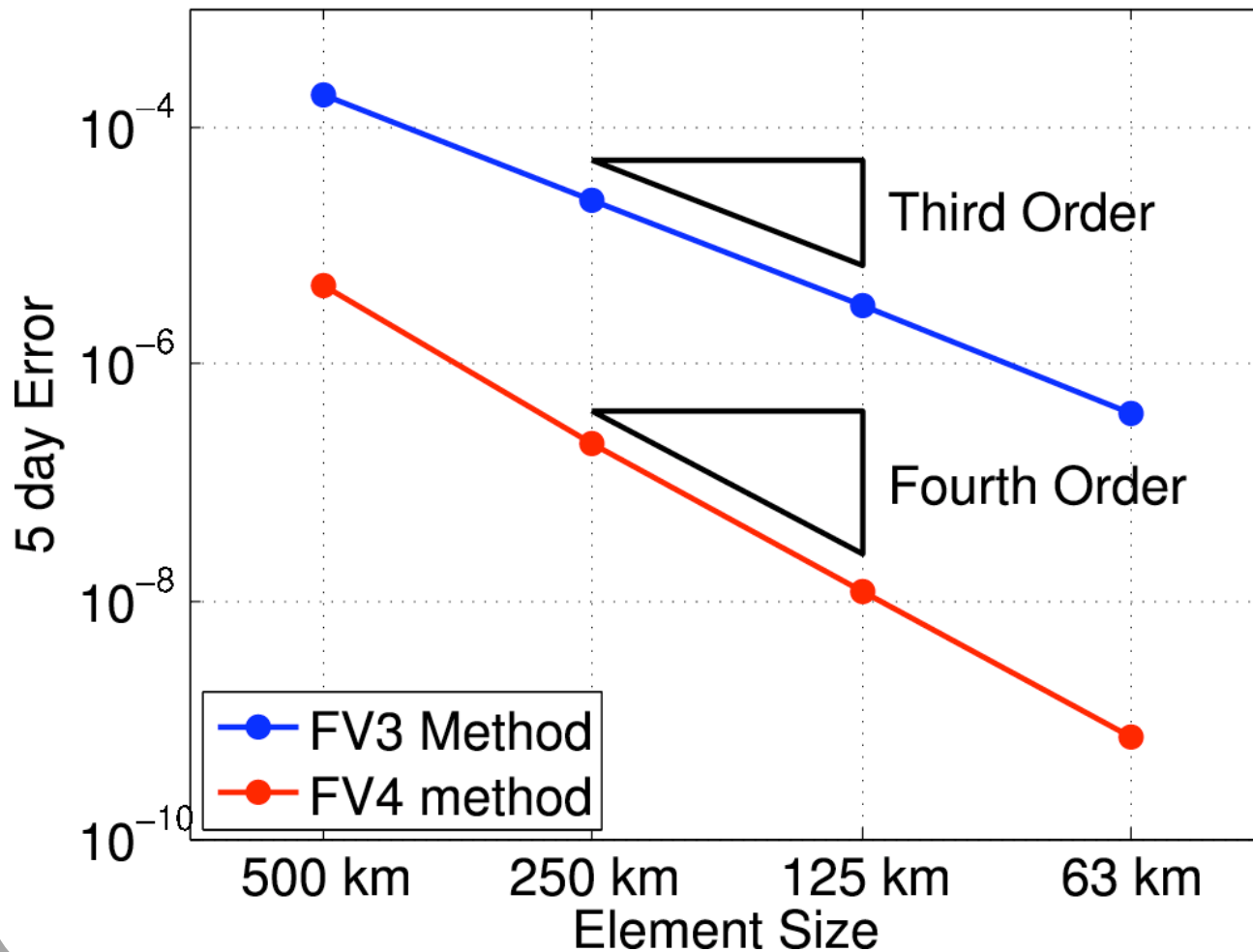
# Numerical Results

Williamson et al. (1992) Test Case 2 - Steady State Geostrophic Flow ( $\alpha=45^\circ$ )



# Numerical Results

Error Convergence: Williamson Test Case 2



Comparisons  
at 250 km  
resolution:

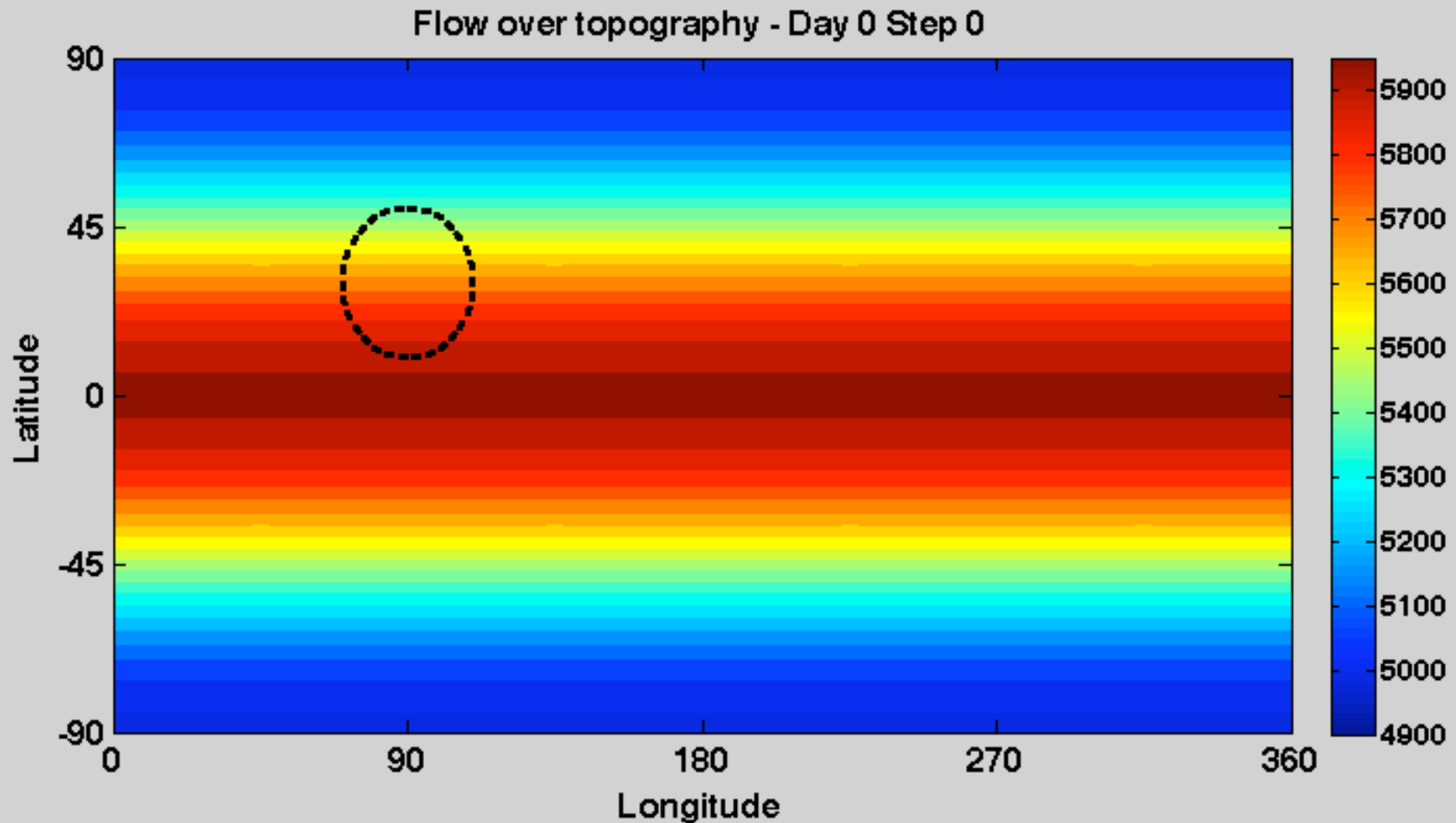
FV PPM:  
 $5 \times 10^{-4}$

SEM (6<sup>th</sup> order):  
 $1.4 \times 10^{-5}$

from St-Cyr,  
Jablonowski, et al.  
(MWR, 2008)

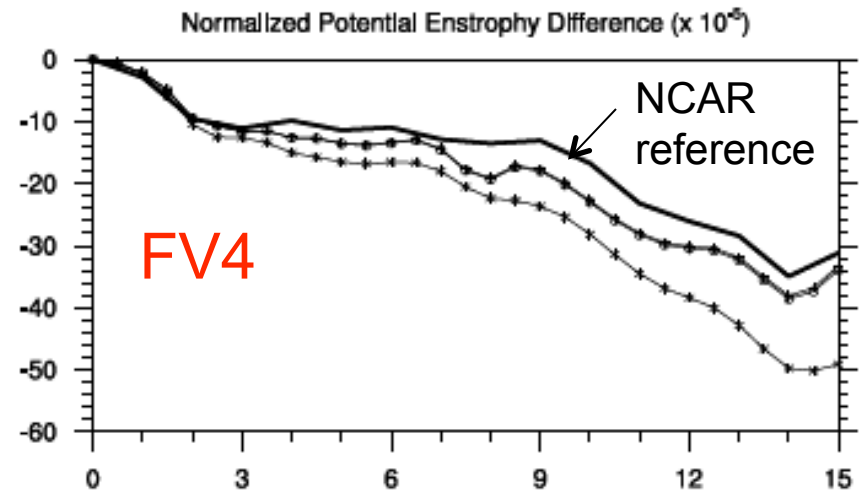
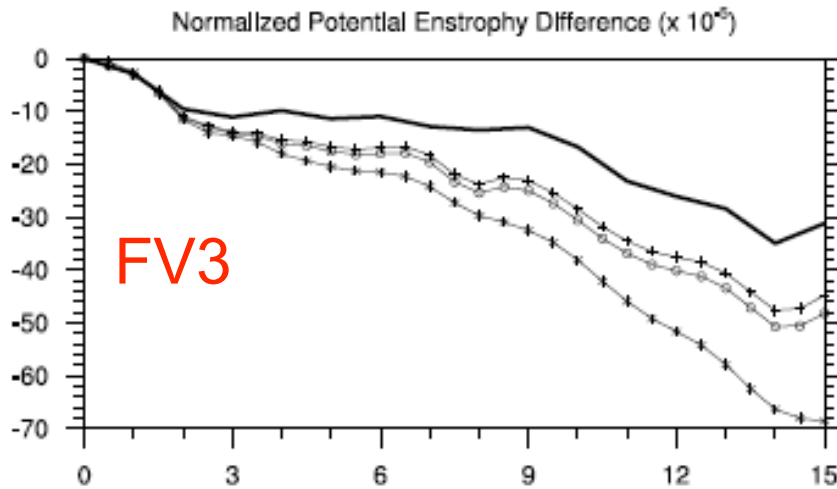
# Numerical Results

Williamson et al. (1992) Test Case 5 - Flow over Topography, 250 km grid

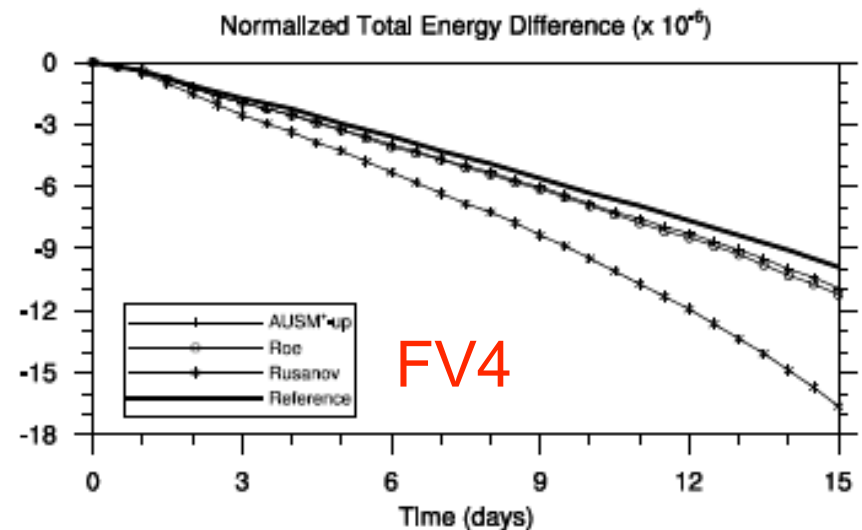
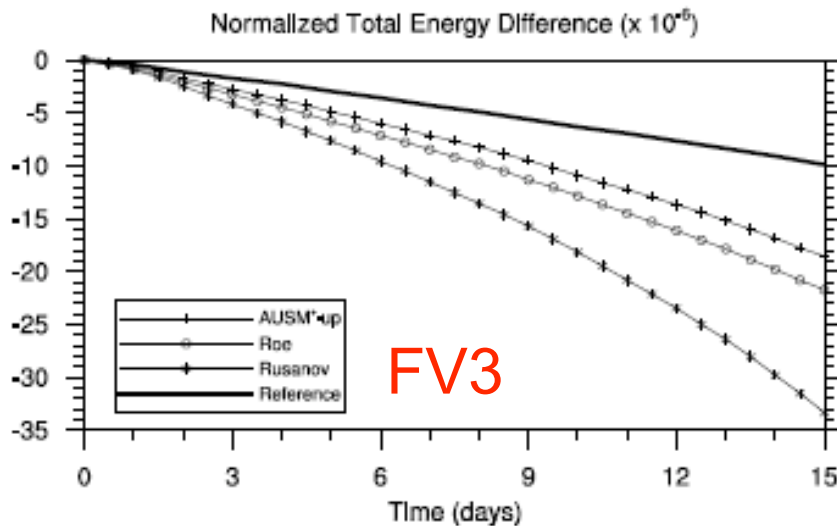


# Test 5: Conservation Properties

Normalized Enstrophy and Total Energy error, 250 km grid



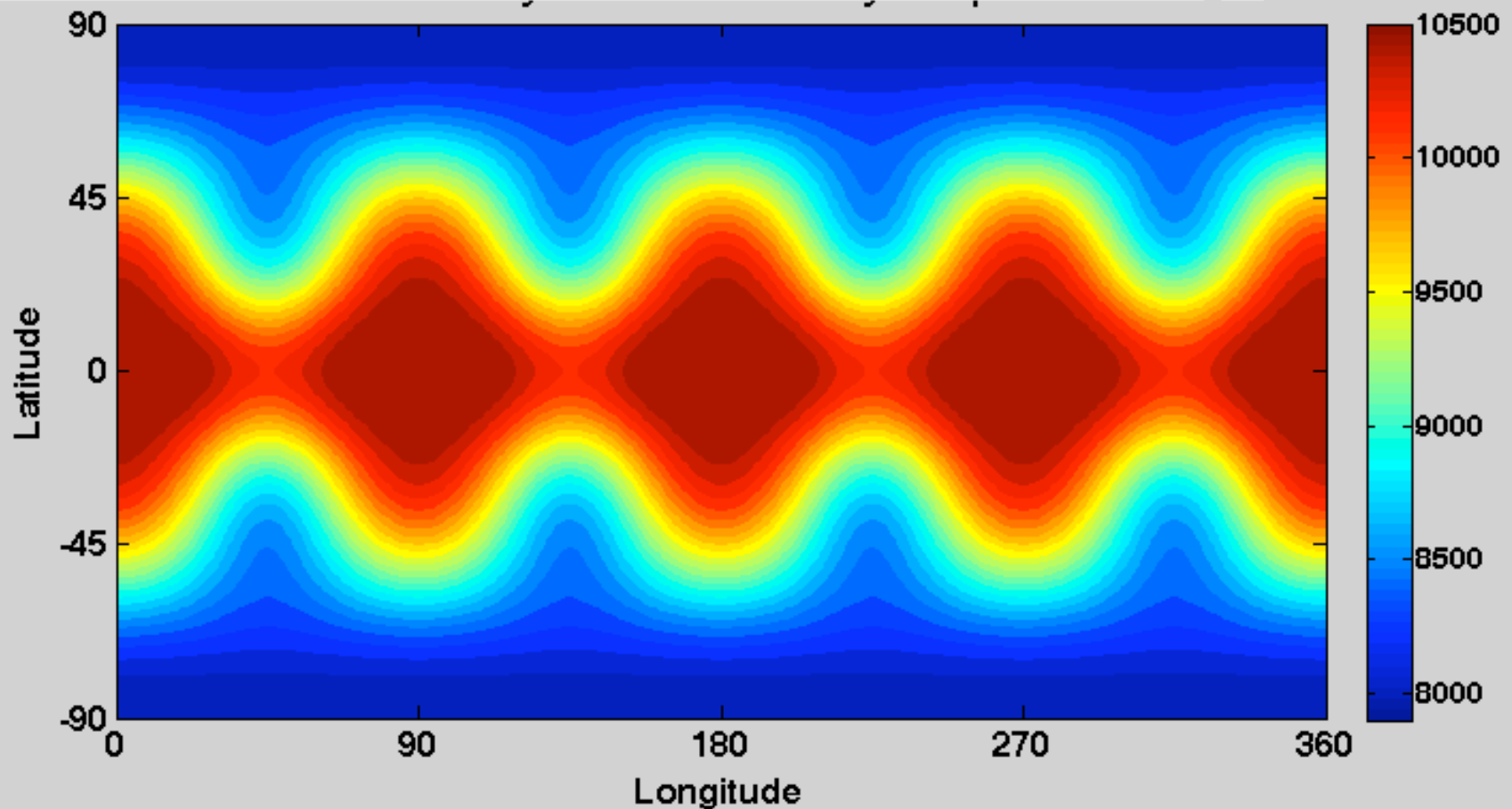
Conservation properties improve at higher order & with better Riemann solvers



# Numerical Results

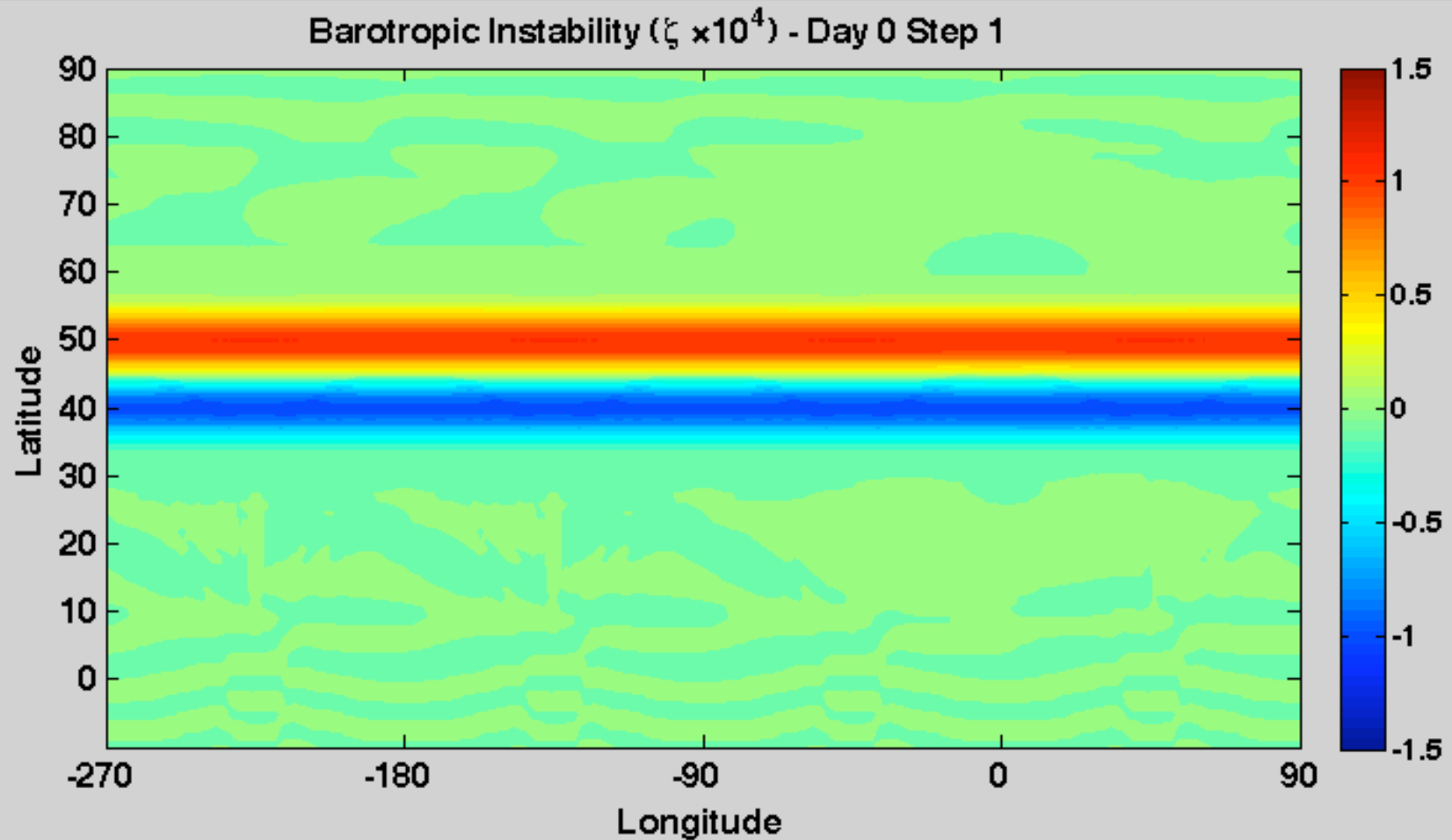
Williamson et al. (1992) Test Case 6 - Rossby-Haurwitz Wave, 125 km grid

Total Fluid Depth (H)



# Numerical Results

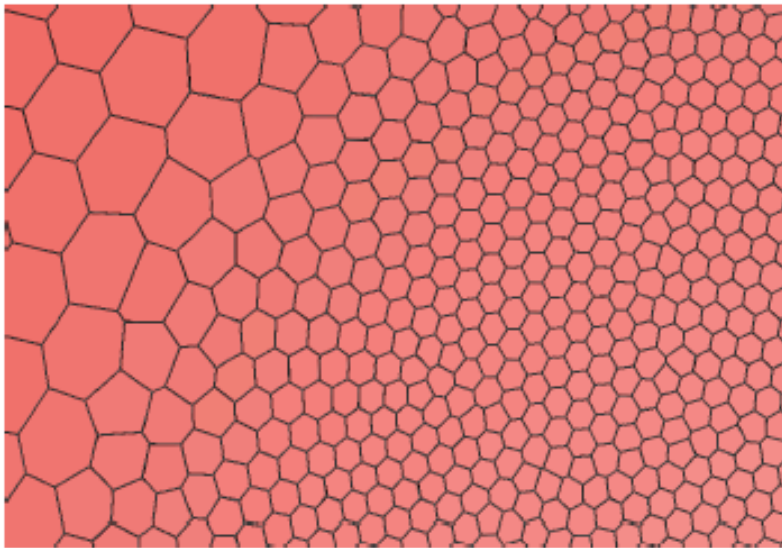
Galewsky et al. (2004) - Barotropic Instability - Vorticity Field  $\zeta$ , 83 km grid



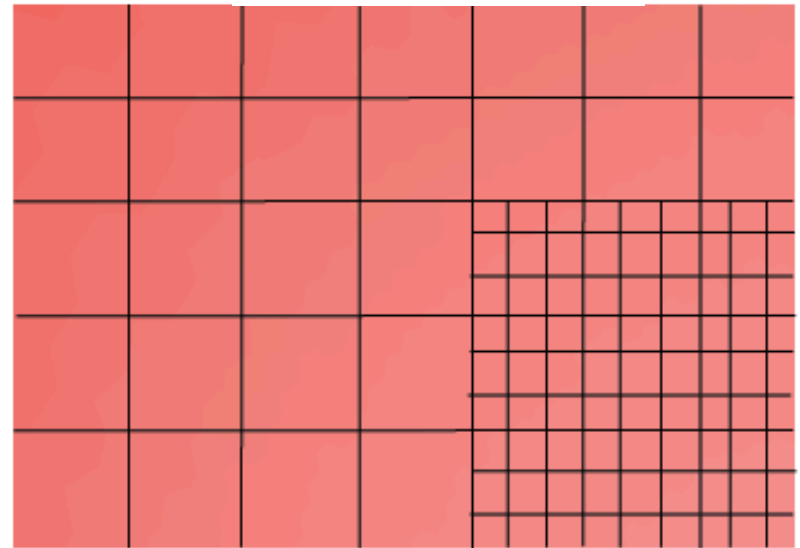
# Variable Resolution

- Allows us to built in regional models in GCMs
- There are many approaches to variable resolution.
- This week we already saw conforming and non-conforming configurations, e.g. in Mark's or Todd's talk (figure is borrowed) :

conforming

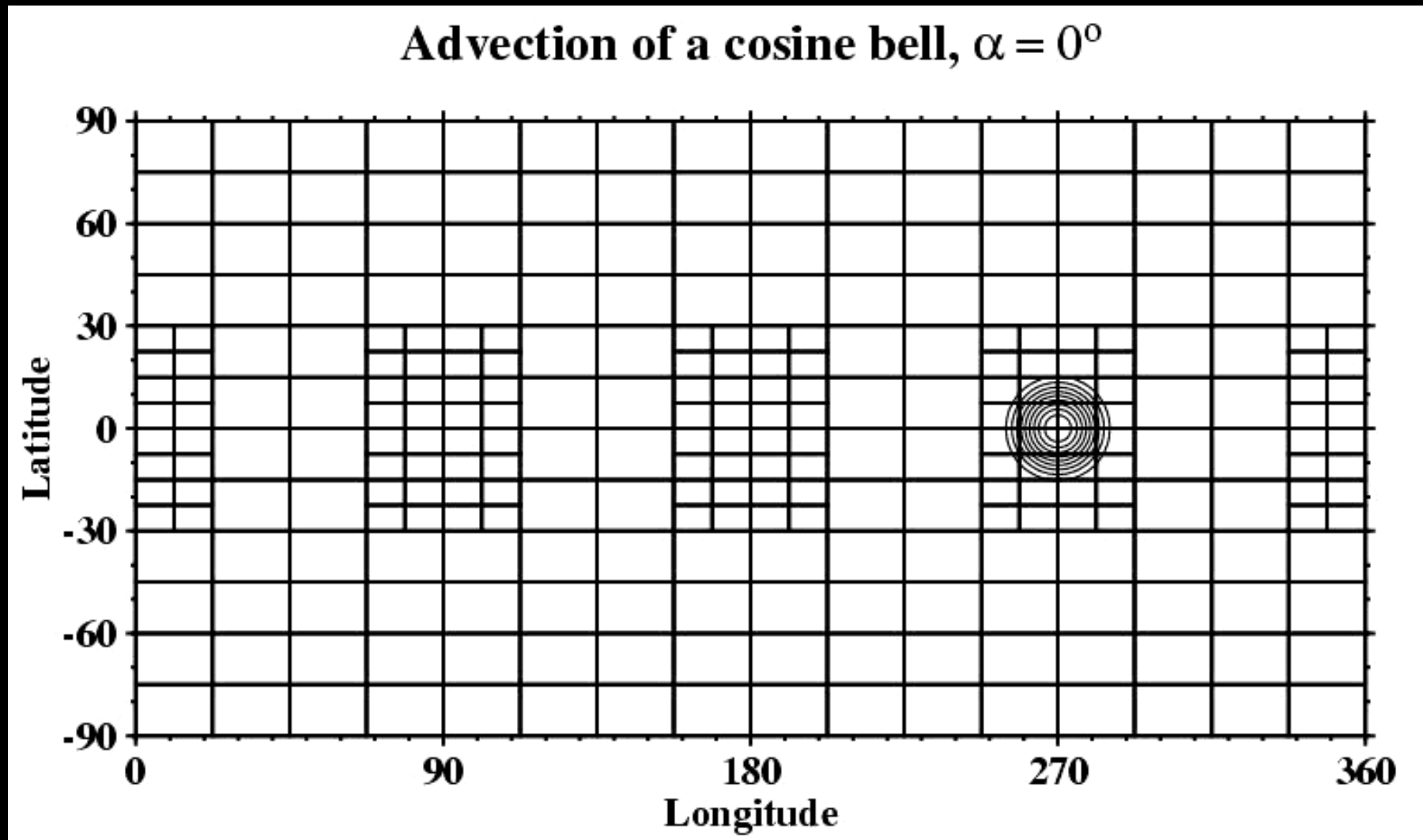


non-conforming



- We want to assess what the variable resolution does to the waves (reflections, distortions, etc.) in non-conforming grids.

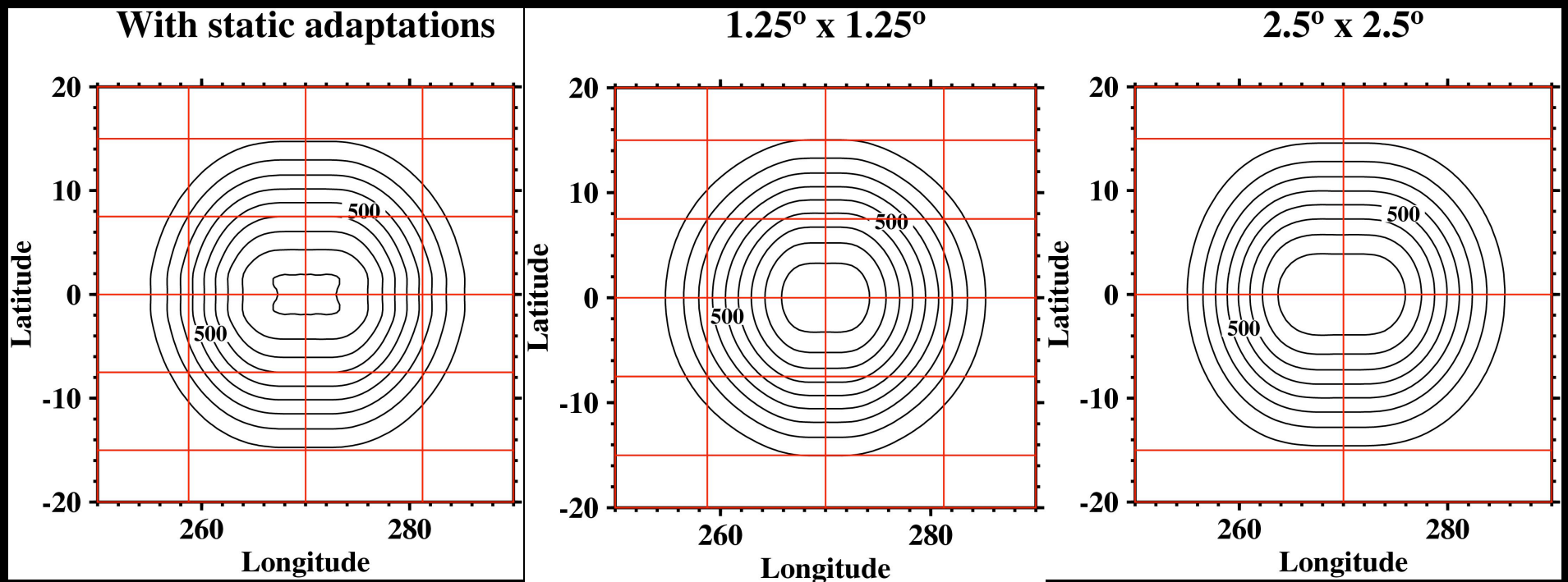
# Adaptive Advection: Deformations?



Block-structured FV (shallow water, advection): test case 1

# Adaptive Advection: Cosine bell at day 12

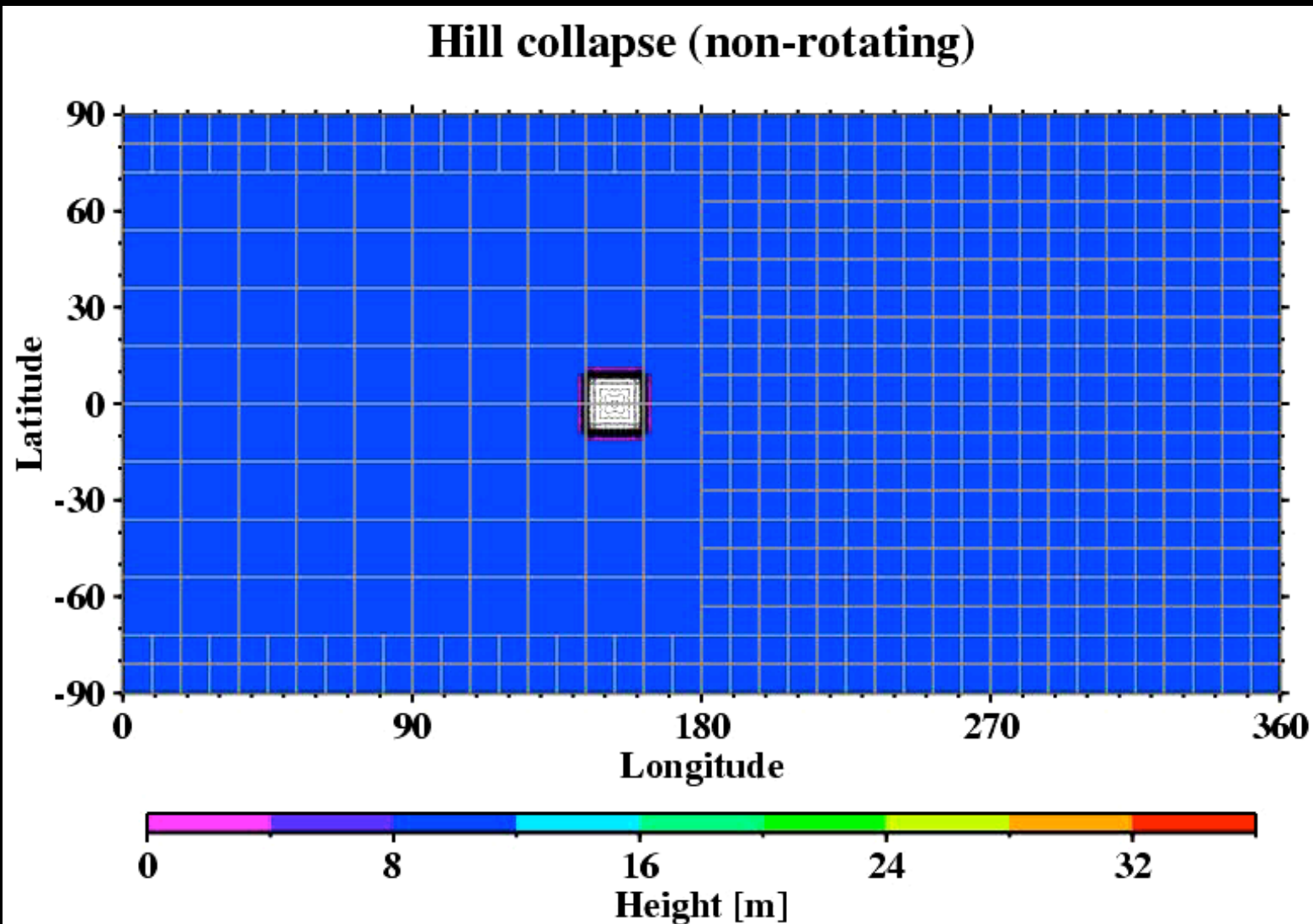
Static adaptations lead to an improved peak amplitude that also changes shape.



Block-structured FV (shallow water, advection): test case 1

# Wave reflections & deformations at interfaces

- Gravity wave test on a non-rotating sphere with fine-coarse grid interface ( $2.5^\circ$  left side,  $1.25^\circ$  right side), 5 days

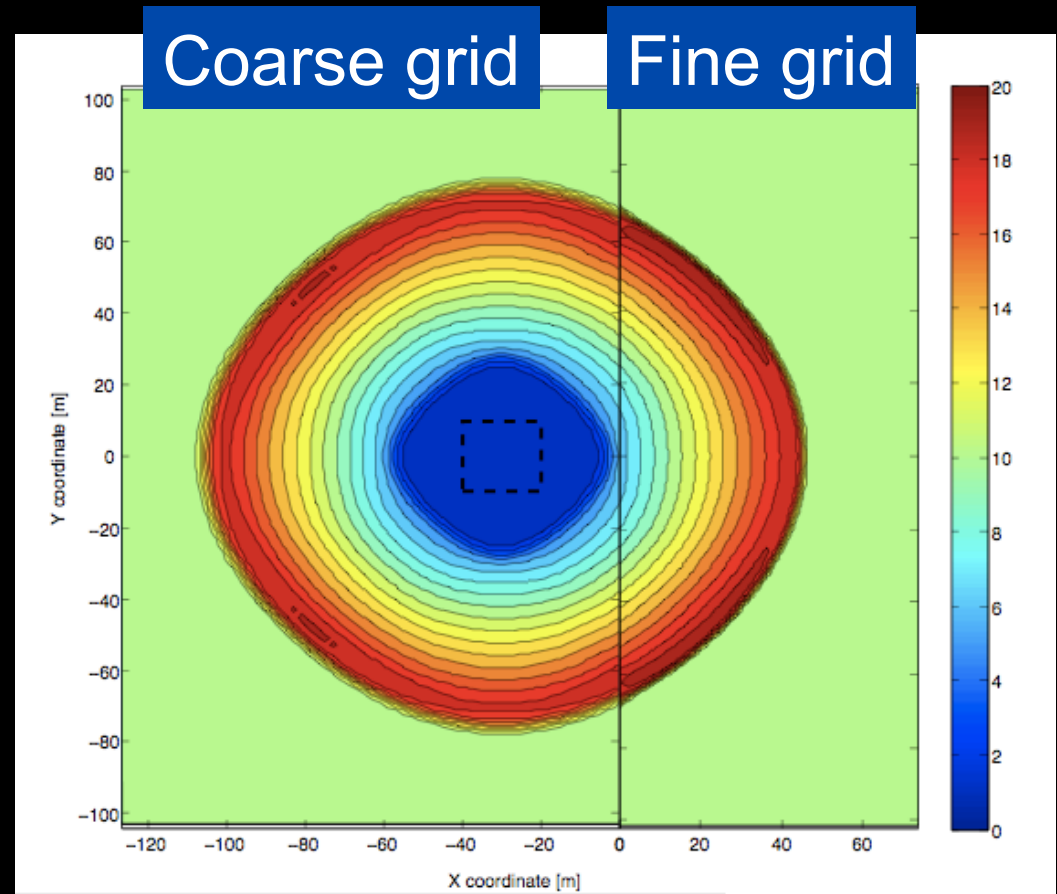


# Wave reflections & deformations at interfaces

- The hill collapse in Cartesian geometry shows almost identical behavior.
- Slightly different phase speeds in the two domains.
- Amplitude losses in the coarse domain.

Composite of the height field of the gravity wave:

- Left: solution on a uniform coarse grid
- Right: Solution on a uniform fine grid

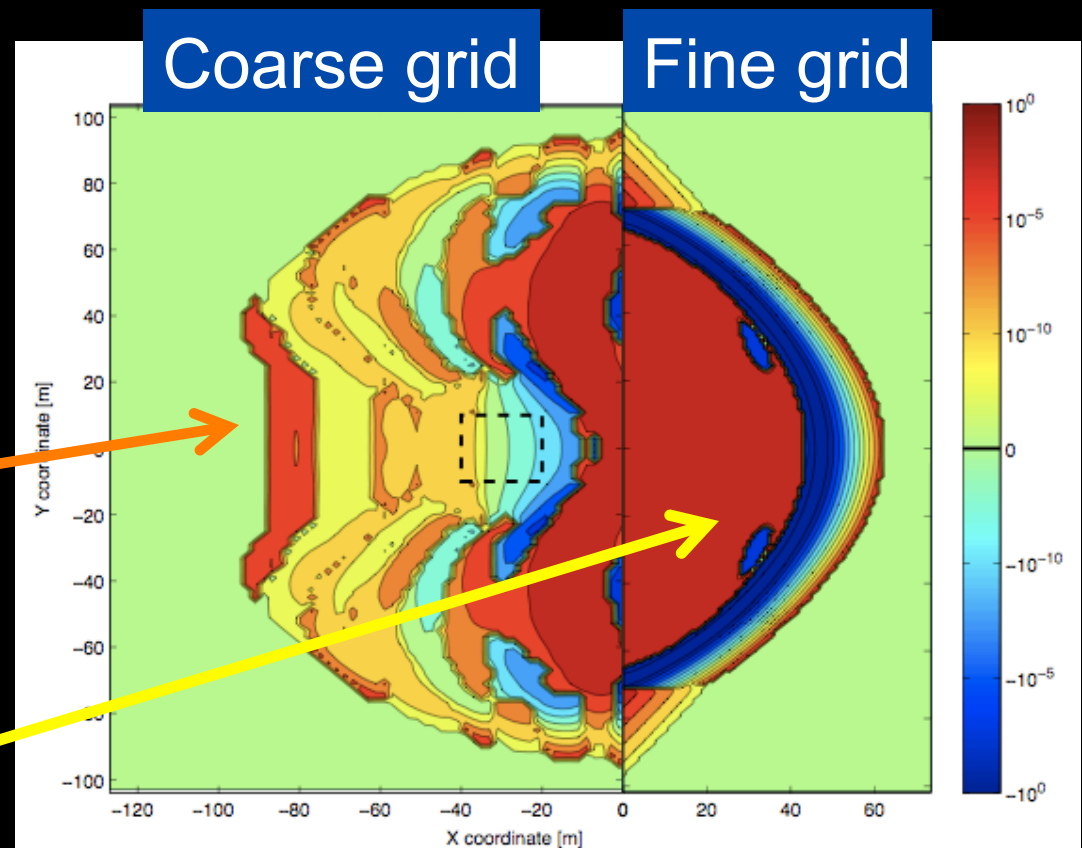


# Errors: Wave reflections and deformations

- The mixed-resolution run is compared to the uniform resolution runs on each side (reference).
- Enhanced logarithmic scale: negative deviations are blue, positive deviations are red.

## Composite of the height error:

- Left: error on the coarse grid due to reflections
- Right: error on the fine grid due to differing wave speeds



# Grid Reflections in Nested Domains

- Easiest approach: assess monochromatic wave in the linear 1D shallow water equations
- Domain has a non-conformal jump in the resolution
- Recently, Harris and Durran (MWR, in press) assessed grid reflections using a symmetric (centered) finite difference method on a C-grid with and without sponges (as in the WRF model), zero energy dissipation.
- In 2009, John Thuburn worked on this topic with his student David Long (M.S. thesis, University of Exeter)
- Frank and Reich (CWI Tech. Report, 2004) investigated spurious wave reflection on staggered grids, found spurious physical mode due to coupling of Riemann invariants
- We assess symmetric and upwind FV method (dissipative) on an A-grid **without sponges** (Ullrich and Jablonowski, JCP, in review)

# Linear 1D SW equations

- Equation set:

$$\frac{\partial h'}{\partial t} + \frac{\partial m'}{\partial x} = 0$$

$$\frac{\partial m'}{\partial t} + gH \frac{\partial h'}{\partial x} = 0$$

$h'$  : height perturbation

$m' = (uh)'$  : momentum perturbation

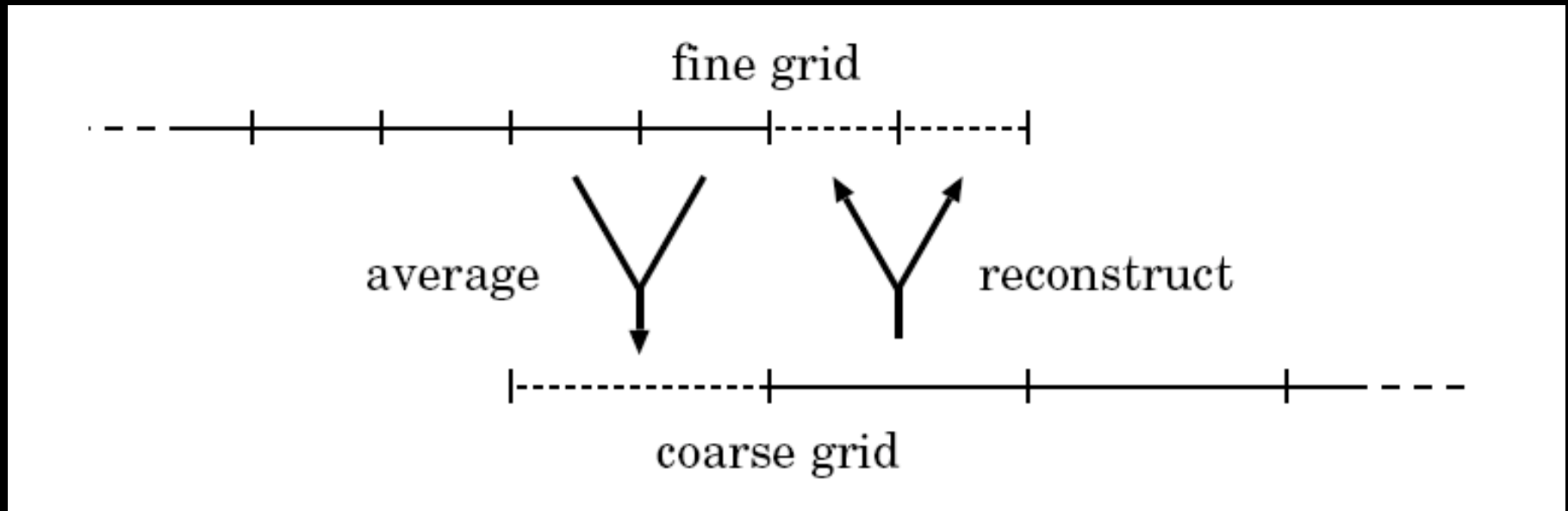
$\sqrt{gH}$  : wave speed

- Admits left-going Riemann invariant  $L'$  and right-going Riemann invariant  $R'$  with evolution equations:

$$\frac{\partial L'}{\partial t} - \sqrt{gH} \frac{\partial L'}{\partial x} = 0 \quad \text{and} \quad \frac{\partial R'}{\partial t} + \sqrt{gH} \frac{\partial R'}{\partial x} = 0$$

# Linear 1D SW equations

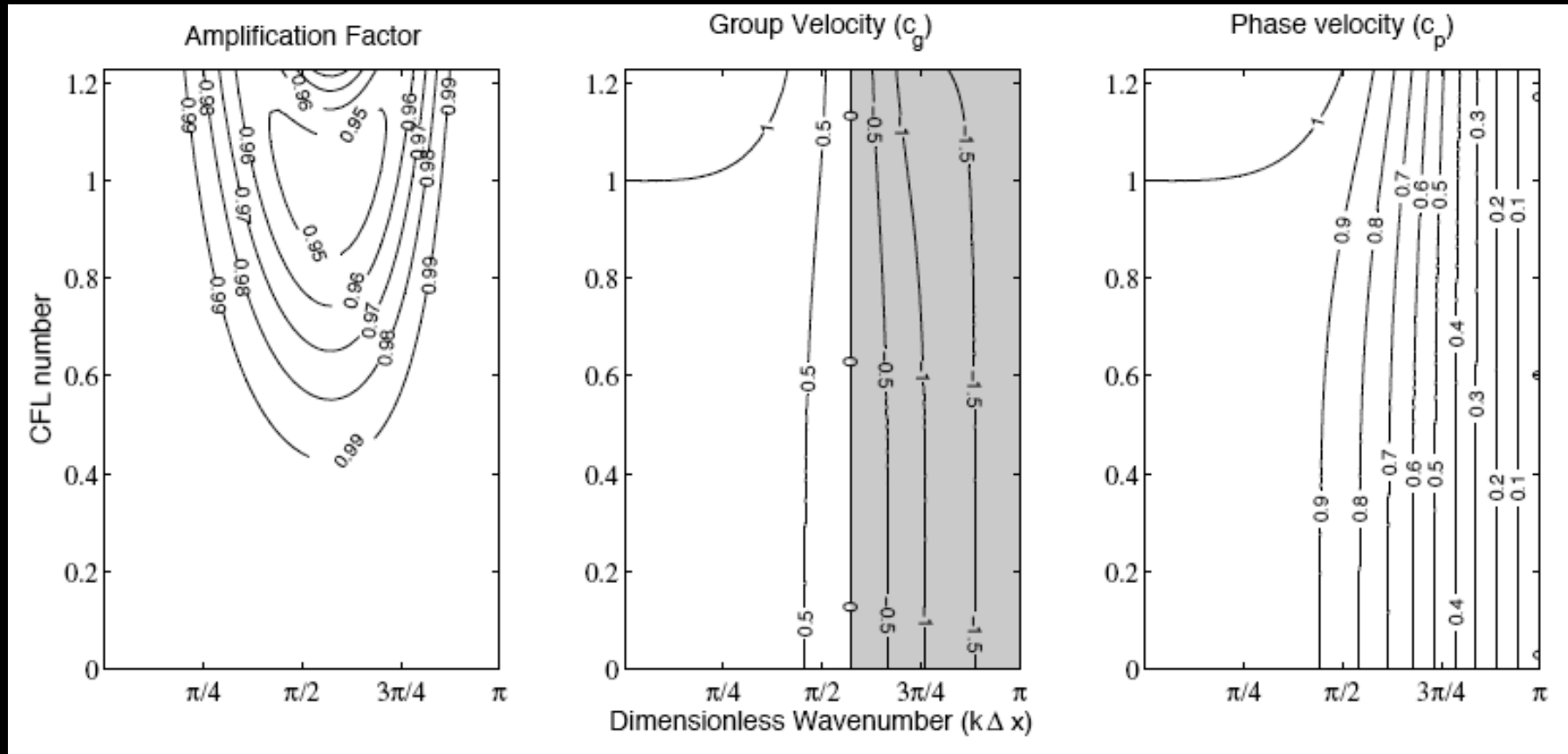
- Introduce jump in the resolution



- Investigate the amplification factor, group speed and phase velocity of discretized FV schemes:
  - Symmetric PPM method with RK3
  - Van-Leer type 3<sup>rd</sup>-order upwind method (FV3p3) with RK3
- Test wave reflection properties: wavemaker experiments

# Amplification Factor, Group & Phase Speeds

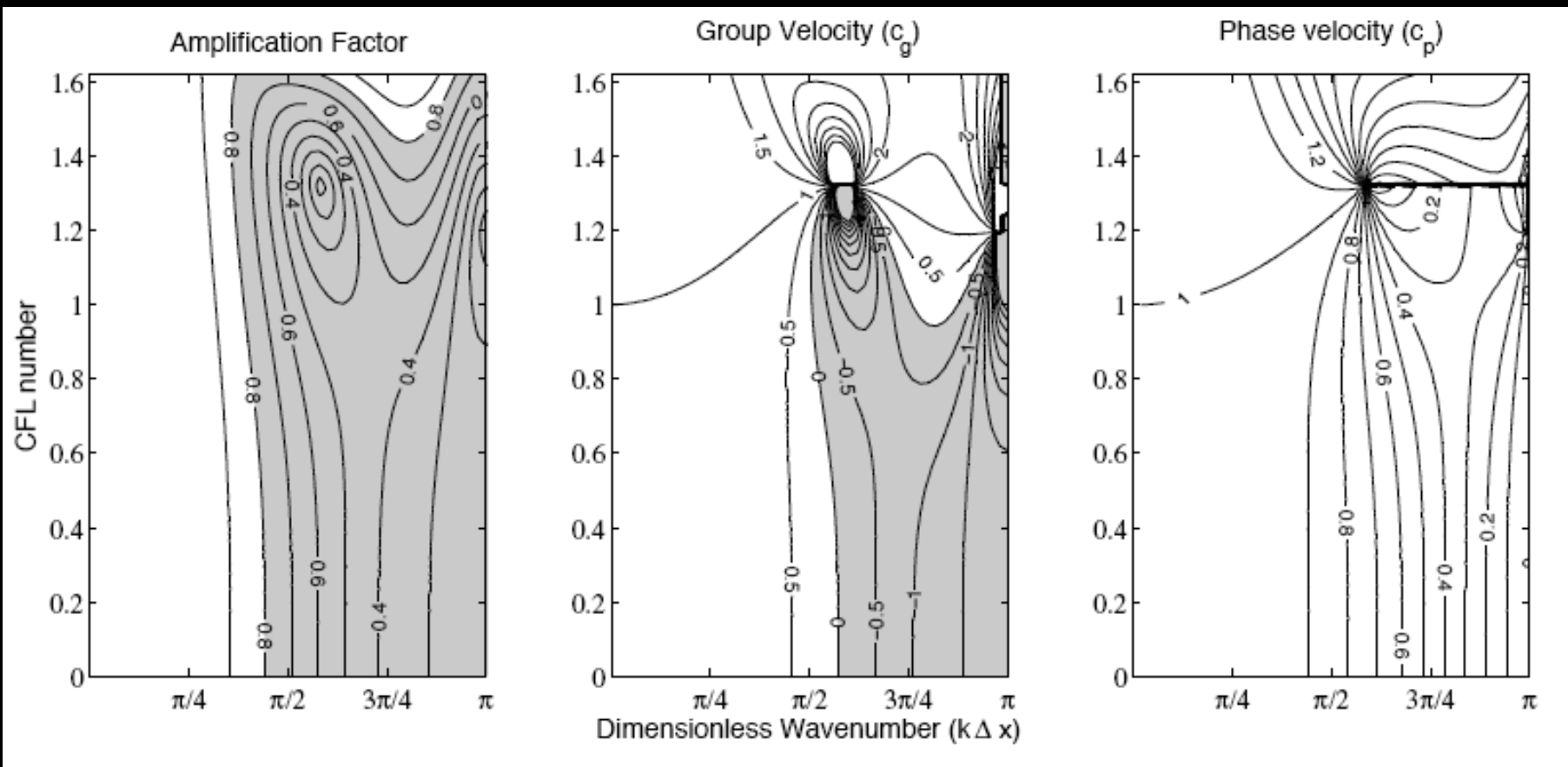
- Example for PPM:



- Negative group speeds in the range  $4\Delta x - 2\Delta x$ , waves travel backward, not damped. Standing  $2\Delta x$  mode present ( $c_p=0$ ).

# Amplification Factor, Group & Phase Speeds

- Example for FV3p3 scheme:

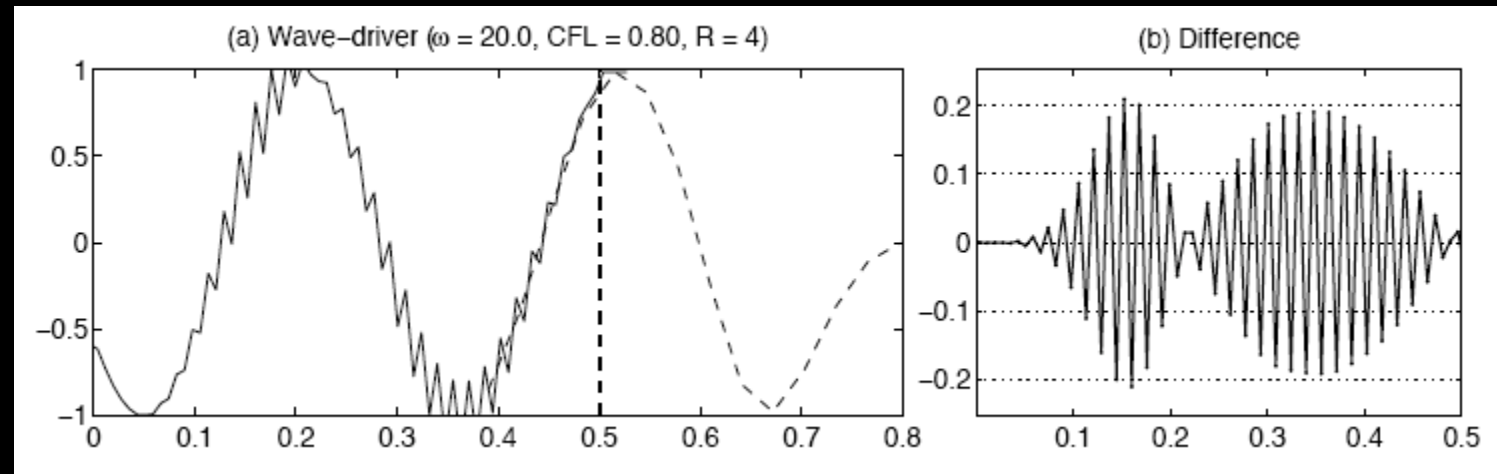


- Negative group speeds in the range  $4\Delta x - 2\Delta x$ , waves travel backward, but are highly damped (amplification factor  $< 0.8$ ).

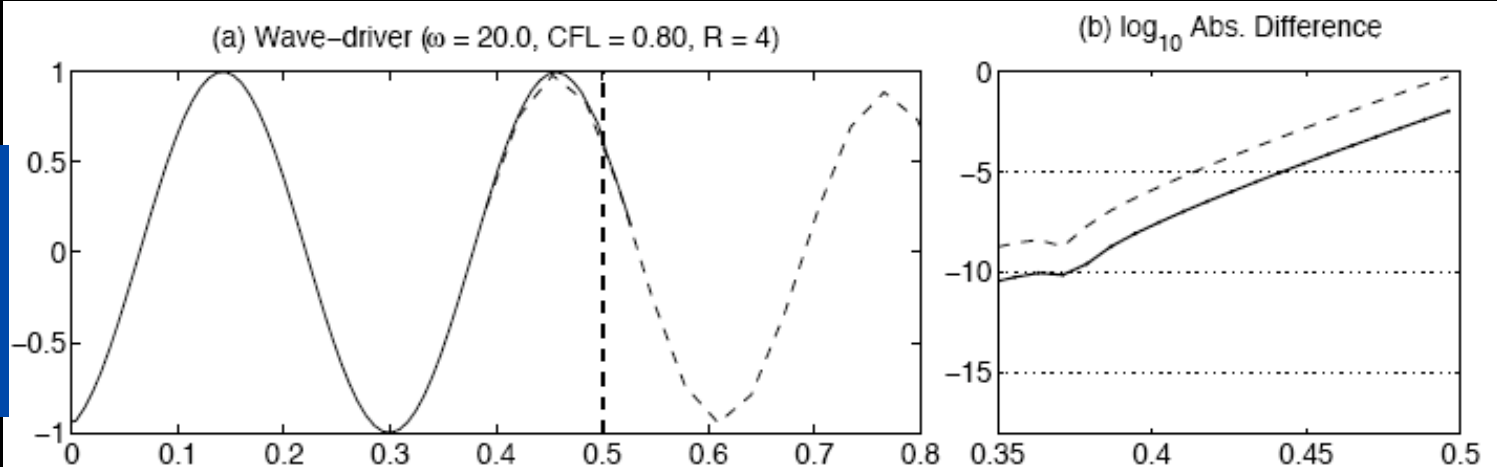
# Wave Reflection Results: PPM & FV3p3

- Examples with **piecewise constant reconstruction** at refinement boundary for well-resolved wave, jump by factor  $R=4$ :

PPM  
(undamped  
parasitic  
mode)



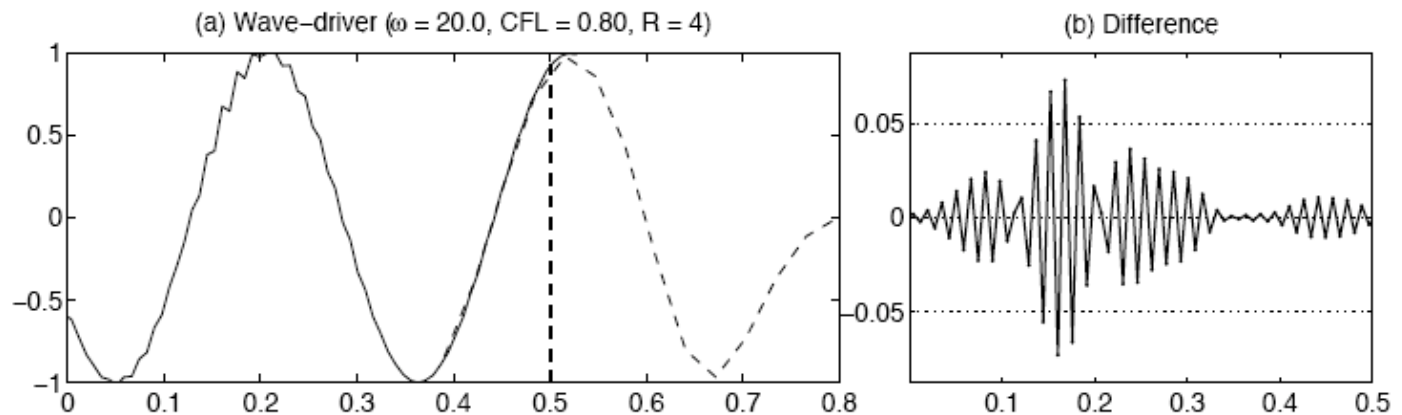
FV3p3  
(reflections  
are diffused)



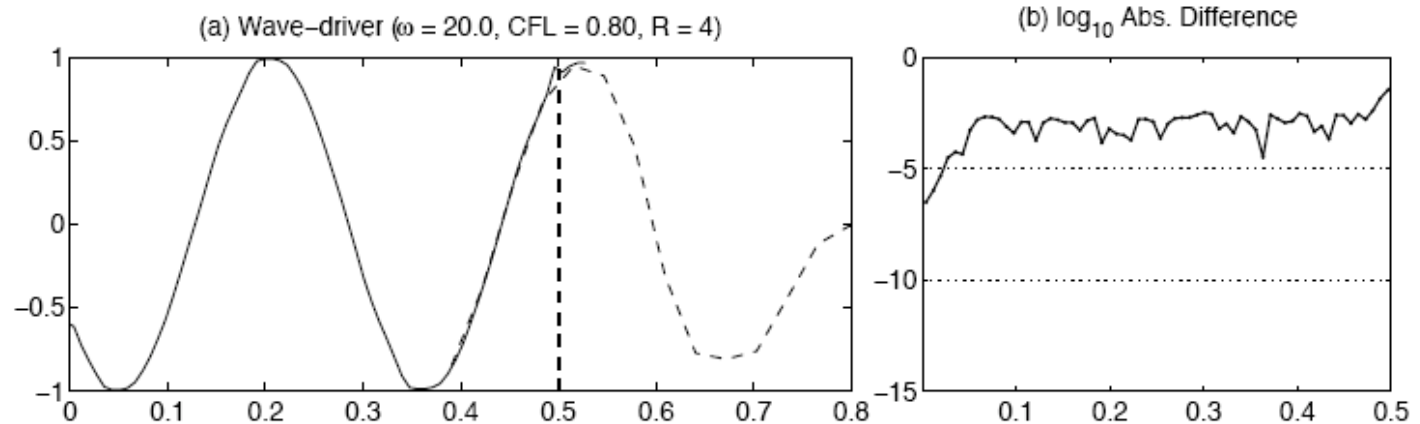
# Wave Reflection Results: PPM

- The symmetric PPM scheme can be improved (here **parabolic reconstruction at grid interface**), but small parasitic mode remains and is persistent.

PPM, no limiter

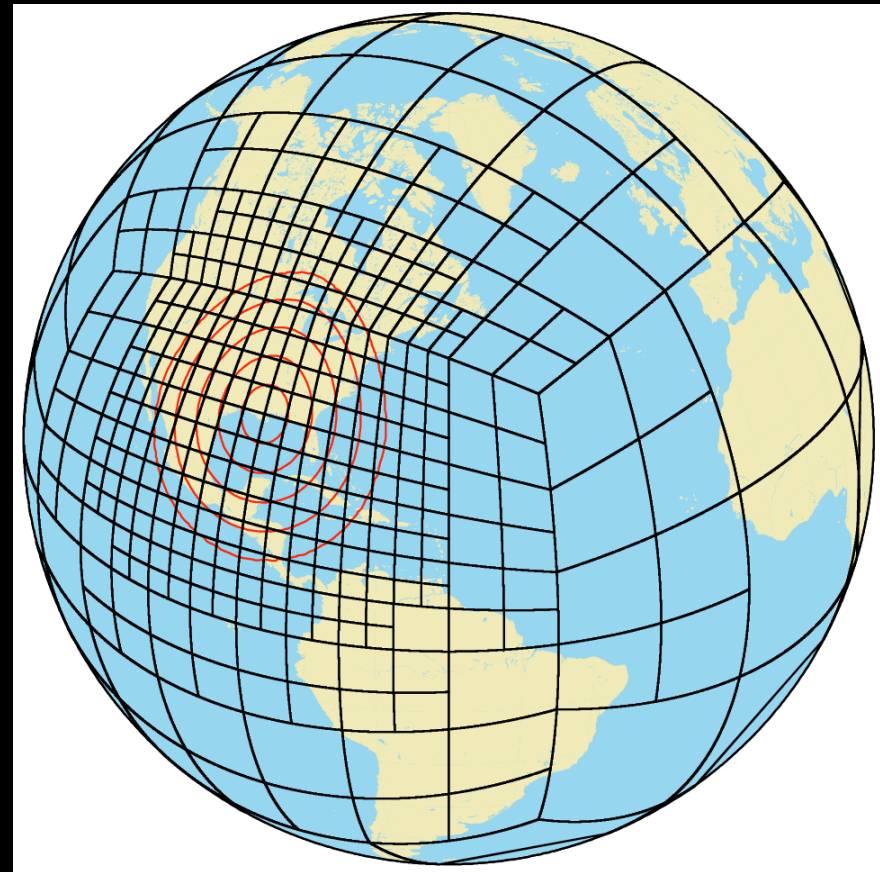


PPM with slope limiter



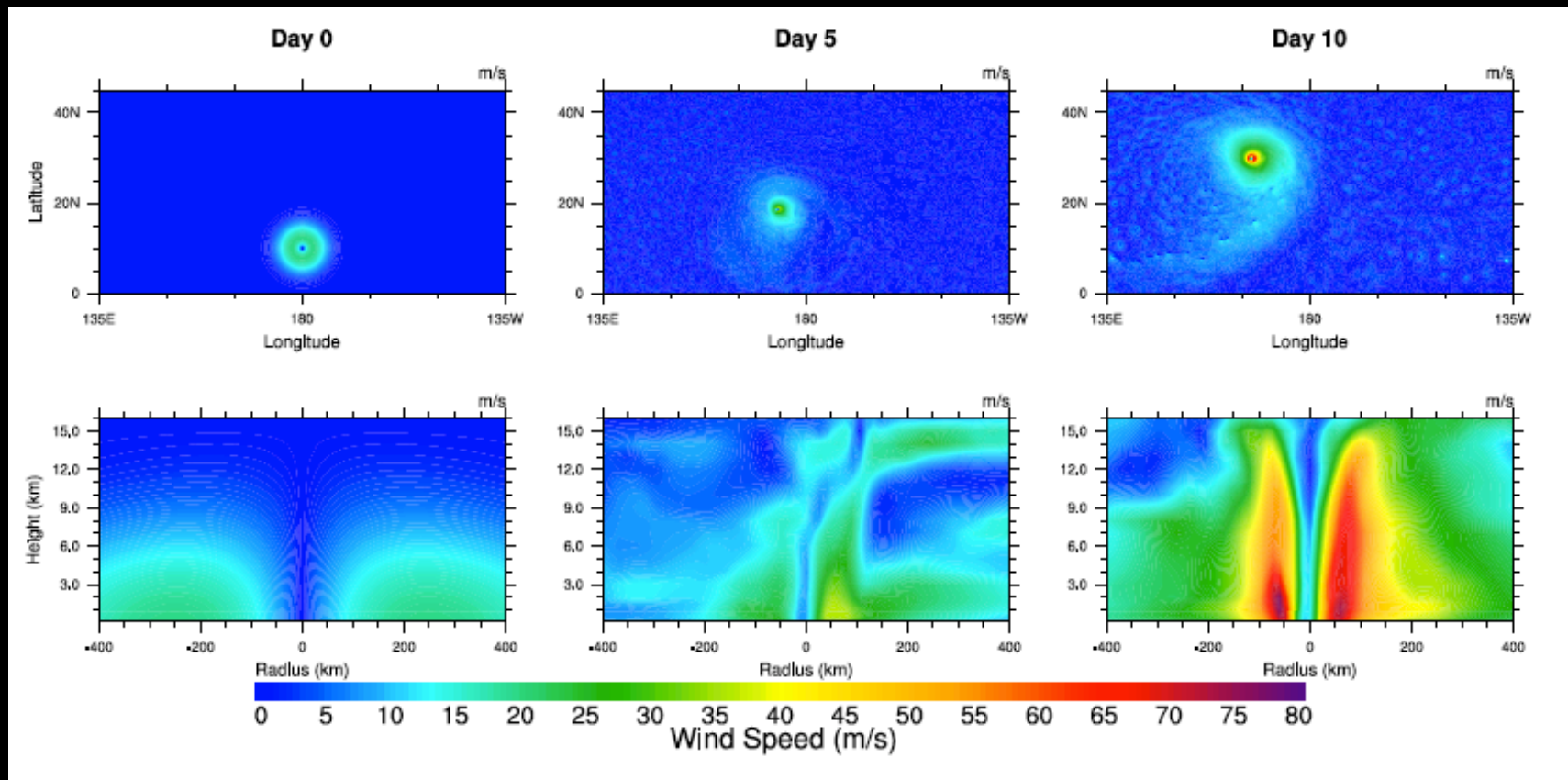
# Target : AMR Dynamical Core on a Cubed-Sphere Grid

- Collaboration with Phil Colella (LBNL), use of the Chombo library
- Cubed-sphere grid
- Non-conforming block-adaptive approach
- 4<sup>th</sup>-order Finite Volume
- RK4 with sub-cycling in refined domains
- Highly scalable



# Outlook: Tropical Cyclone Tests

- Spin-up of idealized tropical cyclone-like vortex in aqua-planet experiments, here in CAM3.1-FV at  $0.125^\circ$  L26 (14 km) resolution



- This year Kevin Reed and I will talk about this work at the AMS Hurricane Conference, High-resolution GCM Workshop at CSU, and 'PDEs on the Sphere Workshop' in Potsdam.

# Summary

- We have successfully demonstrated the use of two high-order finite volume methods for the shallow water equations on the sphere.
- This approach can be extended to a full atmospheric model, e.g. using an IMEX-RK time stepping scheme (Frank's talk), maybe floating Lagrangian coordinates in the vertical.
- The cubed sphere grid avoids problems associated with polar singularities on the regular latitude-longitude grid, and so is a good candidate for general flow problems on the sphere.
- Higher-order is vital for non-conforming AMR applications where the accuracy reduces by one order at refinement boundaries.
- Grid reflections or distortions must be better understood.
- Grid reflections at refinement boundaries are damped out on an unstaggered grid with upwind FV method (due to numerical diffusion). Results suggest that the reflections on the A grid are smaller than the ones on staggered grids.

# References

Ullrich, P. A., C. Jablonowski and B. van Leer: High-order finite-volume methods for the shallow water equations on the sphere. *J. Computational Physics*, revised on 4/15/2010

Ullrich, P. A. and C. Jablonowski: An analysis of finite-volume methods for smooth problems on refined grids. *J. Computational Physics*, in review

Reed, K. A. and C. Jablonowski: An analytic bogus vortex initialization technique for idealized tropical cyclone studies in AGCMs. To be submitted to *Monthly Weather Review*.